Hypoxia-inducible factor 1 is a master regulator of breast cancer metastatic niche formation

Carmen Chak-Lui Wong[a,b], Daniele M. Gilkes[a,b], Huafeng Zhang[a,c,d], Jasper Chen[a,b], Hong Wei[a,b], Pallavi Chaturvedi[a,b], Stephanie I. Fraley[e], Chun-Ming Wong[f,g], Ui-Soon Khoo[g], Irene Oi-Lin Ng[f,g], Denis Wirtz[e], and Gregg L. Semenza[a,b,c,1]

[a]Vascular Program, Institute for Cell Engineering, [b]McKusick–Nathans Institute of Genetic Medicine, and [c]Department of Oncology, The Johns Hopkins University School of Medicine, Baltimore, MD 21205; [e]Department of Chemical and Biomolecular Engineering, The Johns Hopkins University, Baltimore, MD 21218; [f]State Key Laboratory for Liver Research and [g]Department of Pathology, Li Ka shing Faculty of Medicine, University of Hong Kong, Hong Kong; and [d]School of Life Science, University of Science and Technology of China, Hefei, Anhui, China

Contributed by Gregg L. Semenza, August 17, 2011 (sent for review July 25, 2011)

Primary tumors facilitate metastasis by directing bone marrow-derived cells (BMDCs) to colonize the lungs before the arrival of cancer cells. Here, we demonstrate that hypoxia-inducible factor 1 (HIF-1) is a critical regulator of breast cancer metastatic niche formation through induction of multiple members of the lysyl oxidase (LOX) family, including LOX, LOX-like 2, and LOX-like 4, which catalyze collagen cross-linking in the lungs before BMDC recruitment. Only a subset of LOX family members was expressed in any individual breast cancer, but HIF-1 was required for expression in each case. Knockdown of HIF-1 or hypoxia-induced LOX family members reduced collagen cross-linking, CD11b$^+$ BMDC recruitment, and metastasis formation in the lungs of mice after orthotopic transplantation of human breast cancer cells. Metastatic niche formation is an HIF-1–dependent event during breast cancer progression.

extracellular matrix | lung metastasis

Intratumoral hypoxia is a common finding that is attributable to inadequate O_2 delivery to regions of rapidly growing cancers that are distant from functional blood vessels (1). Reduced O_2 availability leads to increased activity of hypoxia-inducible factors (HIFs), which consist of an O_2-regulated HIF-1α or HIF-2α subunit and the constitutively expressed HIF-1β subunit (2, 3). HIF inhibition blocks tumor xenograft growth (2, 4).

Metastasis is responsible for 90% of deaths among patients who have breast cancer and involves multiple steps, including cancer cell invasion through ECM, intravasation, extravasation, and colonization of distant organs (5). Recent studies have reported that prior recruitment of bone marrow-derived cells (BMDCs) to the metastatic site promotes subsequent colonization by cancer cells (6). The primary tumor is responsible for BMDC recruitment to the metastatic site. Breast tumors secrete lysyl oxidase (LOX), which localizes at metastatic sites in the lungs and remodels collagen, thereby facilitating BMDC recruitment (7, 8). LOX oxidatively deaminates the ε-amino groups of lysine residues, resulting in intramolecular and intermolecular cross-linking of collagen molecules (9). Cross-linking stabilizes collagen by assembly into fibrils and fibers, which enhance ECM tensile strength, leading to focal adhesion formation and PI3K signaling (10). The LOX family is composed of LOX and LOX-like (LOXL) proteins LOXL1–4. So far, only LOX has been implicated in metastatic niche formation (7). In this study, we demonstrate that HIF-1 regulates metastatic niche formation by activating expression of LOX and LOXL proteins. HIF-1 silencing suppresses metastatic niche formation and metastasis regardless of which LOX family member is involved.

Results

Hypoxia-Induced LOX/LOXL Expression in Breast Cancer Cell Lines. Two metastatic breast cancer cell lines, MDA-MB-231 (MDA-231) and MDA-MB-435 (MDA-435), as well as a nonmetastatic line, MCF-7, were cultured under standard, nonhypoxic tissue culture conditions of 95% air/5% CO_2 (vol/vol; 20% O_2) and under hypoxic culture conditions of 1% O_2/5% CO_2/94% N_2 (vol/vol/vol; 1% O_2). Each cell line exhibited a different pattern of expression in response to hypoxia (Fig. 1*A* and Fig. S1 *A–C*). In MDA-231, LOX and LOXL4 were induced by hypoxia, whereas in MDA-435, LOXL2 was induced by hypoxia. LOX was hypoxia-induced in MDA-231, as previously reported (8), but not in MDA-435 (Fig. S1*B*). LOXL1 and LOXL3 expression was not induced in either cell type (Fig. S1*C*). LOX/LOXL protein expression was not detectable in MCF-7 (Fig. S1*B*), which is consistent with a critical prometastatic role for LOX family members in breast cancer.

LOX/LOXL Expression in Patients with Breast Cancer. To gain clinical insight into *LOX*, *LOXL2*, and *LOXL4* gene expression in breast cancer, we compared their expression in cancer vs. surrounding normal tissue from the same patient. We observed expression of different combinations of LOX members in the 11 human breast cancers that were analyzed (Fig. 1*B*). LOX, LOXL2, and LOXL4 mRNA was overexpressed by at least twofold in 7 of 11, 8 of 11, and 2 of 11 cases, respectively (Fig. 1*B*). Thus, multiple LOX family members are up-regulated in different breast cancers.

HIF-Dependent Expression of LOX Family Members. *LOX* gene expression is regulated by HIF-1 in breast cancer cells (8). To test whether HIFs mediate expression of other LOX family members, we generated stable transfectants of MDA-231 and MDA-435 with shRNA-mediated knockdown of HIF-1α (sh-1α), HIF-2α (sh-2α), or double knockdown (DKD) of both HIF-1α and HIF-2α as well as empty vector (EV) transfectants (Fig. S1 *D* and *E*). Hypoxic induction of LOX and LOXL4 mRNA and protein expression was suppressed when HIF-1α, HIF-2α, or both were knocked down in MDA-231 (Fig. 1*C* and Fig. S1 *F* and *G*). In MDA-435, hypoxic induction of LOXL2 was blocked only when HIF-1α was knocked down (Fig. 1*D*).

***LOXL4* Is an HIF Target Gene.** LOX and LOXL2 were shown to be direct targets of HIF-1 (8, 11). To examine whether *LOXL4* is an HIF-1 target, we searched for the HIF binding site consensus sequence 5′-RCGTG-3′ (12). Two copies were present as an inverted repeat within intron 1 (Fig. S2*A*). ChIP assays in MDA-231 demonstrated hypoxia-inducible binding of HIF-1α, HIF-2α, and HIF-1β to this DNA sequence (Fig. 2 *A–C*) but not at the *RPL13A* gene (Fig. *S2B*), which is not HIF-regulated. To verify that HIF-1 and HIF-2 were binding to a functional hypoxia response element (HRE), a 60-bp sequence spanning the HIF binding sites (HRE-WT; Fig. S2*A*) was inserted into reporter plasmid pGL2-promoter, in which a basal SV40 promoter drives firefly luciferase expression. A second construct was generated in

Author contributions: C.C.-L.W., D.M.G., and G.L.S. designed research; C.C.-L.W., D.M.G., H.Z., J.C., H.W., P.C., S.I.F., C.-M.W., U.-S.K., and I.O.-L.N. performed research; D.W. contributed new reagents/analytic tools; C.C.-L.W., D.M.G., and G.L.S. analyzed data; and C.C.-L.W. and G.L.S. wrote the paper.

The authors declare no conflict of interest.

[1]To whom correspondence should be addressed. E-mail: gsemenza@jhmi.edu.

This article contains supporting information online at www.pnas.org/lookup/suppl/doi:10.1073/pnas.1113483108/-/DCSupplemental.

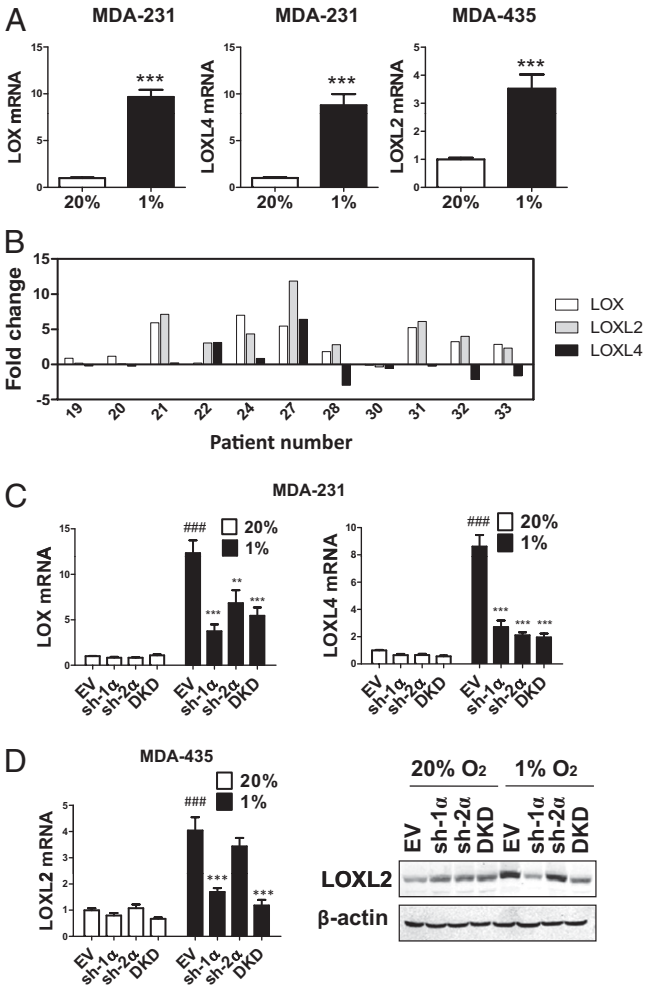

Fig. 1. LOX/LOXL expression in breast cancer cell lines and in patients who have breast cancer. (*A*) MDA-231 and MDA-435 were cultured in 20% or 1% O_2 for 24 h. LOX/LOXL mRNA levels were analyzed by real-time RT-qPCR relative to 18S rRNA, and ratios were normalized to results obtained at 20% O_2. ***$P < 0.001$ vs. 20% O_2, Student *t* test (mean ± SEM; $n = 3$). (*B*) LOX/LOXL mRNA levels were analyzed by RT-qPCR (relative to 18S rRNA) in breast cancer tissue and surrounding normal tissue. The fold-increased expression of each target mRNA in cancer compared to normal tissue was determined by the threshold cycle (C_T) method, in which $\Delta C_T = C_{T,\ target} - C_{T,\ 18S}$ and $\Delta\Delta C_T = \Delta C_{T,\ cancer} - C_{T,\ normal}$. (*C*) LOX and LOXL4 mRNA were analyzed in MDA-231 subclones. (*D*) LOXL2 mRNA and protein levels were analyzed in MDA-435 subclones. ###$P < 0.001$ vs. 20% O_2-EV; **$P < 0.01$, ***$P < 0.001$ vs. 1% O_2-EV; one-way ANOVA with Bonferroni correction (mean ± SEM; $n = 3$).

which both HIF sites were mutated (HRE-Mut; Fig. S2*A*). In MDA-231 cells transfected with pGL2-HRE-WT, luciferase activity increased 2.5-fold on hypoxic exposure, whereas in cells transfected with pGL-HRE-Mut, hypoxic induction of luciferase was impaired (Fig. 2*D*). Thus, ChIP and transcription assays demonstrate that *LOXL4* is a direct HIF target gene.

HIF-Dependent LOX/LOXL Expression Leads to Collagen Remodeling. To explore the effect of HIF on collagen cross-linking, we incubated type I collagen with conditioned medium (CM) generated by hypoxic or nonhypoxic MDA-231 subclones and imaged fibrillar collagen by reflection confocal microscopy (Fig. 3*A*). CM from hypoxic MDA-231-EV cells stimulated prominent collagen cross-linking (Fig. 3*A*). This hypoxia-induced effect was abolished in DKD cells, demonstrating the importance of HIF-1α and HIF-2α expression for collagen cross-linking (Fig. 3*A*).

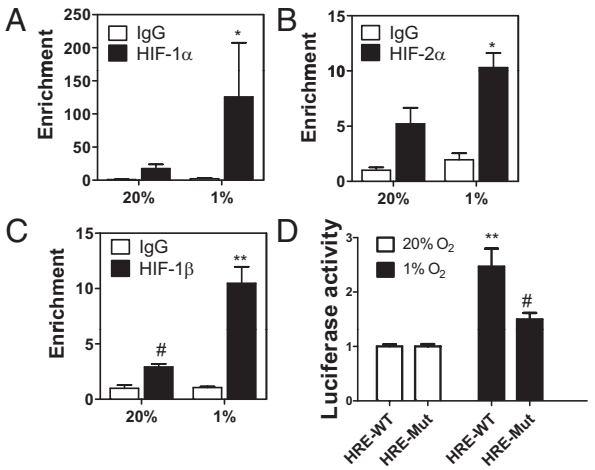

Fig. 2. *LOXL4* is an HIF target gene. (*A–C*) MDA-231 cells were incubated in 20% or 1% O_2 for 4 h. ChIP assay was performed using IgG, HIF-1α, HIF-2α, or HIF-1β antibodies. *LOXL4* intron 1 primers were used for qPCR, and values were normalized to 20% O_2-IgG. *$P < 0.05$ vs. 1% IgG or 20% HIF-α, **$P < 0.01$ vs. 1% IgG or 20% HIF-1β, #$P < 0.05$ vs. 20% IgG; Student *t* test on log-converted values (mean ± SEM; $n = 3$). (*D*) WT and Mut HRE sequences were inserted into firefly luciferase vector pGL2-promoter and cotransfected with *Renilla* luciferase vector into MDA-231 cells, which were incubated at 20% or 1% O_2 for 24 h. The Firefly/*Renilla* ratio was calculated and normalized to value for 20% O_2. **$P < 0.01$ vs. 20% O_2 HRE-WT, #$P < 0.05$ vs. 1% O_2 HRE-WT; Student *t* test (mean ± SEM; $n = 3$).

Because LOX and LOXL4 were induced by hypoxia in MDA-231, whereas LOXL2 was induced by hypoxia in MDA-435, we generated stable transfectants expressing shRNA against LOX (shLOX) or LOXL4 (shLOXL4) in MDA-231 (Fig. S3 *A* and *B*) and against LOXL2 (shLOXL2) in MDA-435 (Fig. S3*C*) and nontargeted control (NTC) subclones. Type I collagen incubated with CM from knockdown subclones exhibited reduced cross-linking, with respect to both fiber size and number, compared with CM from NTC cells (Fig. 3 *B* and *C* and Fig. S4 *A–C*). Thus, expression of HIFs and multiple LOX family members is important for collagen fiber formation.

HIF-Dependent LOX/LOXL Expression Preconditions ECM for Bone Marrow Cell Invasion. Invasion of BMDCs at the metastatic site is required for metastatic niche formation. To study the effect of cancer cells on BMDC invasion, we coated transwell filters in migration chambers with matrigel (tumor-derived ECM), incubated the matrigel with CM, and seeded bone marrow cells (BMCs) on top (Fig. S4*D*). Matrigel that was treated with CM from hypoxic MDA-231-EV cells stimulated increased BMC invasion compared with CM from nonhypoxic cells, and the effect of hypoxia was lost when HIF-1α or HIF-2α expression was knocked down (Fig. 3*D*). BMC invasion was also enhanced when matrigel was pretreated with CM from hypoxic MDA-435 cells, and this effect was abrogated in sh-1α and DKD cells but not in sh-2α cells (Fig. 3*E*). This result is consistent with our finding that HIF-1α (but not HIF-2α) regulates LOXL2 expression in MDA-435 and suggests that LOXL2 plays a critical role in collagen remodeling and metastatic niche formation in MDA-435. CM from MDA-231-shLOX and -shLOXL4 cells did not induce BMC invasion compared with MDA-231-NTC cells, under hypoxic conditions (Fig. 3*F*). Fewer BMCs invaded through matrigel pretreated with CM of hypoxic MDA-435-shLOXL2 cells compared with hypoxic MDA-435-NTC cells (Fig. 3*G*). Thus, the HIF → LOX/LOXL pathway in breast cancer cells is important for ECM remodeling that facilitates BMC invasion.

HIF Is Required for Breast Cancer Cells to Precondition Lungs for BMDC Recruitment. To determine whether HIF-1α or HIF-2α is

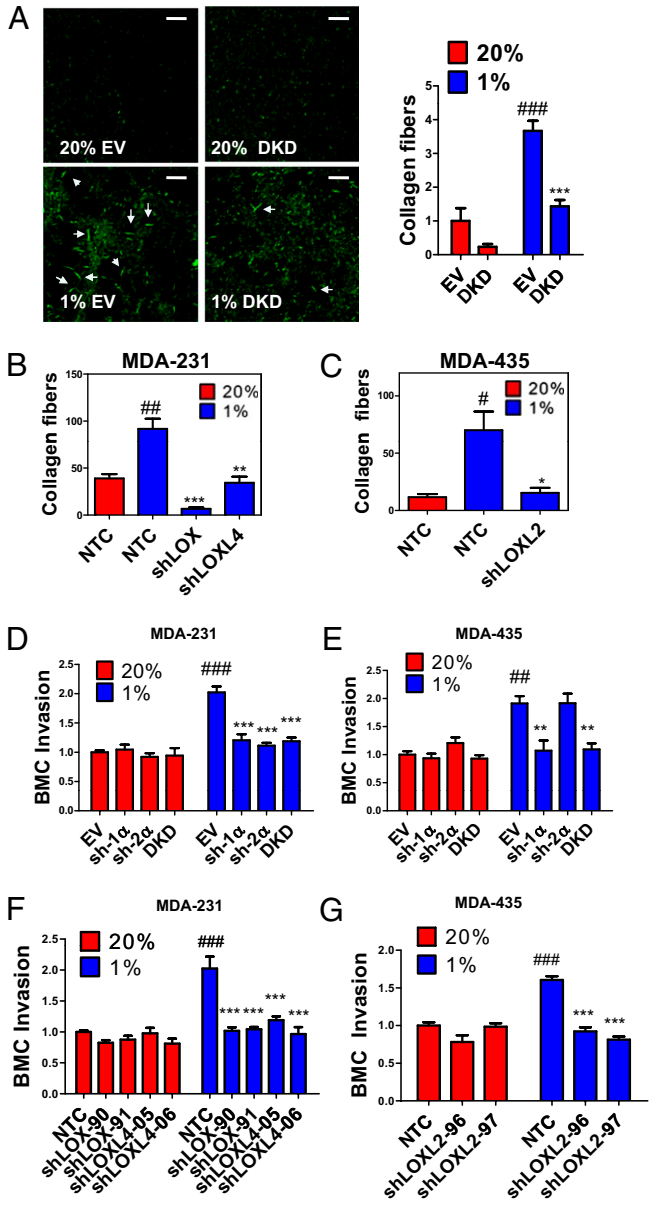

Fig. 3. HIFs and LOX/LOXL proteins regulate collagen cross-linking and BMC invasion. (*A–C*) Collagen gel was mixed with CM generated from indicated MDA-231 and MDA-435 subclones that were cultured in 20% or 1% O_2. Collagen fibers were counted in at least three random fields. Results were normalized to 20% O_2 controls. (*D–G*) Transwell filters coated with matrigel were incubated with CM from breast cancer cells for 16 h at 37 °C. BMCs in serum-free medium were seeded in the top chamber. Medium containing 10% FBS was placed in the bottom chamber. BMCs that invaded through the matrigel to the bottom chamber were counted and normalized to the 20% O_2 control (EV or NTC). $^{\#\#}P < 0.01$, $^{\#\#\#}P < 0.001$ vs. 20% O_2 control (EV or NTC); $^{*}P < 0.05$, $^{**}P < 0.01$, $^{***}P < 0.001$ vs. 1% O_2 control (EV or NTC); one-way ANOVA with Bonferroni correction (mean ± SEM; $n = 3$).

required for metastatic niche formation, we orthotopically implanted MDA-231 subclones into the mammary fat pad (MFP) of SCID mice. The lungs were harvested 3 wk later, and Picrosirius Red-stained sections were analyzed under polarized light to identify cross-linked collagen fibrils. Cross-linking was decreased in the lungs of mice implanted with sh-1α, sh-2α, or DKD cells compared with EV cells (Fig. 4*A*), indicating that HIF-1α and HIF-2α expression in MDA-231 regulates collagen remodeling in the lungs of tumor-bearing mice. We then analyzed BMDC recruitment to the lungs by flow cytometry. MDA-231-sh-1α, -sh-2α, and -DKD tumors recruited fewer $CD11b^+CD45^+$ cells (denoted $CD11b^+$ BMDCs) to the lungs compared with EV tumors (Fig. 4*B*). Immunohistochemical analysis of the lungs of EV and DKD tumor-bearing mice confirmed the results of flow cytometry analysis (Fig. 4*C*). We also orthotopically implanted MDA-435 subclones and harvested the lungs 45 d after injection. Knockdown of HIF-1α but not HIF-2α reduced tumor growth, collagen remodeling, $CD11b^+$ BMDC recruitment, and metastasis (Fig. 4 *D–G*). Thus, HIF-1 activity in breast cancer cells is critical for metastatic niche formation.

LOXL2 and LOXL4 Are Required for Metastatic Niche Formation by MDA-435 and MDA-231. To assess the functional role of individual LOX members, we injected MDA-435-NTC and -shLOXL2 cells into the MFP of mice and monitored BMDC recruitment and lung metastasis. There was no significant difference in primary tumor growth between NTC and shLOXL2 subclones (Fig. 5*A*). However, less cross-linked collagen (Fig. 5*B* and Fig. S5*A*) and fewer $CD11b^+$ BMDCs (Fig. 5*C* and Fig. S5 *B* and *C*) were found in the lungs of mice carrying shLOXL2 tumors relative to NTC tumors. Histological analysis and qPCR demonstrated decreased metastatic burden in the lungs of mice injected with shLOXL2 cells (Fig. 5*D* and Fig. S5*D*). However, no difference in BMDC recruitment or lung metastasis was observed in mice carrying NTC vs. shLOX tumors (Fig. S5 *E–G*). Thus, only depletion of the hypoxia-induced LOX family member (LOXL2) impaired metastatic niche formation and metastasis of MDA-435 cells.

We also implanted MDA-231-NTC and -shLOXL4 cells into the MFP. Although the growth rates of NTC and shLOXL4 primary tumors were similar (Fig. 5*E*), lungs of mice bearing shLOXL4 tumors displayed a marked reduction in cross-linked collagen (Fig. 5*F* and Fig. S6*A*), $CD11b^+$ BMDCs (Fig. 5*G* and Fig. S6*B*), and lung metastases (Fig. 5*H* and Fig. S6*C*) compared with the lungs of NTC tumor-bearing mice. The effects on collagen crosslinking were observed at both premetastatic (Fig. S6*A*) and metastatic (Fig. S6*D*) sites in the lungs. Knockdown of LOXL4 with a different shRNA or knockdown of LOX recapitulated the results (Fig. S6 *E* and *F*), demonstrating that both LOX and LOXL4 are required for metastatic niche formation by MDA-231 cells.

To image metastases in vivo, we implanted luciferase-expressing MDA-231-NTC and -shLOXL4 cells. There was no difference in the signals generated by primary tumors in the MFP (Fig. S7*A*). However, the lungs of shLOXL4 tumor-bearing mice exhibited a reduction in $CD11b^+$ BMDC cells (Fig. S7*B*) and metastatic breast cancer cells, as demonstrated by qPCR (Fig. S7*C*) and by bioluminescent imaging (Fig. S7*D*). Sensitive bioluminescent imaging also allowed analysis of lymph node metastasis in these mice. We found decreased luminescence of axillary lymph nodes from shLOXL4, compared with NTC, tumor-bearing mice (Fig. S7*E*).

Kinetic Analysis of Metastatic Niche Formation. To delineate the sequential events of metastatic niche formation, we injected MDA-435 cells into the MFP. Mice were euthanized at 8, 16, or 24 d after injection, and lungs were harvested for analysis. Tumor-free (naive) mice were included at each time point as negative controls. Increased collagen cross-linking in the lungs of tumor-bearing mice was observed on day 8 (Fig. 5*I* and Fig. S7*F*), but neither $CD11b^+$ BMDCs nor cancer cells were detected (Fig. S7*G*). On day 16, we detected increased $CD11b^+$ BMDCs in the lungs of tumor-bearing mice (Fig. 5*J* and Fig. S7*H*). qPCR and histology studies confirmed the absence of cancer cells in the lungs (Fig. 5*J* and Fig. S7*I*). On day 24, cancer cells were detected in the lungs (Fig. 5*K* and Fig. S7*J*). This experiment provides a precise timeline of the steps involved in metastatic niche formation by MDA-435 cells, beginning with collagen cross-linking followed by BMDC homing and, finally, cancer metastasis (Fig. 5*L*).

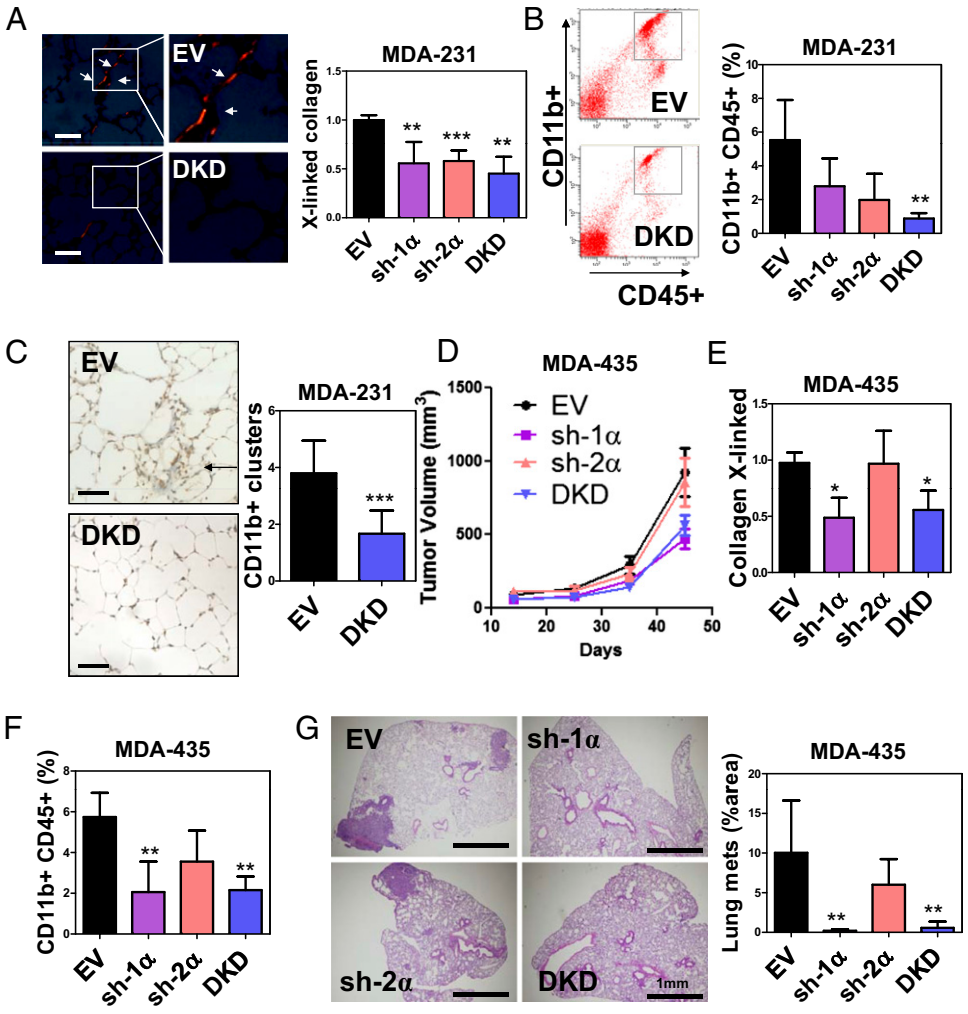

Fig. 4. Inhibition of HIFs in MDA-231 suppresses BMDC homing to the lungs. (*A*) MDA-231 subclones were injected into the MFP of SCID mice. Lungs were harvested on day 24. (*Left*) Representative photomicrographs of Picrosirius Red-stained lungs under polarized light are shown. (Scale bar = 50 μm.) (*Right*) Cross-linked collagen fibers were counted and normalized to EV control. (*B*) Flow cytometry analysis of $CD45^+CD11b^+$ cells in the lungs of tumor-bearing mice. (*C*) (*Left*) Immunohistochemical staining of CD11b in lung sections from mice that received MFP injection of EV or DKD subclone. (Scale bar = 50 μm.) (*Right*) $CD11b^+$ cell clusters were counted at a magnification of 20× in 10 random fields. (*D*) Mice were injected with MDA-435 subclones. Tumor volume (mean ± SD; $n = 4–5$) was plotted against time. The number of cross-linked collagen fibers (normalized to EV) (*E*) and $CD11b^+CD45^+$ BMDCs (*F*) in the lungs (% of total cell number) was determined. (*G*) Percentage of total lung area occupied by metastases was determined by image analysis of H&E-stained sections. $^*P < 0.05$, $^{**}P < 0.01$, $^{***}P < 0.001$ vs. EV; one-way ANOVA, Bonferroni correction (mean ± SD; $n = 4–5$).

Discussion

In this study, we have demonstrated that HIFs are critical regulators of metastatic niche formation through cancer cell-specific transcriptional activation of genes encoding multiple members of the LOX family. Our study highlights three important points. First, the HIF → LOX/LOXL pathway plays a critical role in metastasis in orthotopic models of breast cancer. Traditionally, metastasis is considered to be a late event in cancer progression. In contrast, we demonstrated that initiation of the metastatic process is an early event that is dependent on HIF-1, which is consistent with the association between HIF-1α overexpression and patient mortality that is observed even in patients with early-stage node-negative breast cancers (13). Taken together with the results of the present study, those data suggest that patients with HIF-1α–overexpressing breast cancers may benefit from more intensive therapy, including HIF inhibitors (2).

Second, we demonstrated the benefits of HIF suppression in genetically different breast cancers. The combination of genetic alterations in each breast cancer is unique, and cancer heterogeneity remains a major obstacle to successful therapy. Our analysis of cell lines and primary breast cancers revealed that different breast cancers exhibited different patterns of LOX family expression. Pharmacological inhibition of LOX by β-aminopropionitrile (βAPN) has been reported to inhibit BMDC recruitment and inhibit metastasis in MDA-231 models (8, 14); however, βAPN does not inhibit the activity of all LOX family members, specifically LOXL2 (15). On the other hand, hypoxia is a common feature in cancers (1), and suppression of HIF activity through genetic silencing blocked metastatic niche formation in multiple breast cancer lines, suggesting that HIFs represent a broader target than currently available drugs or antibodies that each target only a subset of LOX/LOXL proteins. Our results highlight the heterogeneous nature of the response to hypoxia, with HIF-1 activating a unique battery of target genes within each breast cancer.

Third, we identified LOXL4 as a direct HIF target gene in breast cancer cells and delineated its role in metastasis. LOXL4, the least well-characterized family member, is overexpressed in head/neck and colorectal carcinomas (16, 17). The HIF → LOXL4 pathway plays a significant role in collagen cross-linking, metastatic niche formation, and metastasis in a subset of breast cancers. LOXL4 also promotes lymph node metastasis, which underscores the multiple cellular and molecular mechanisms by which LOX/LOXL proteins promote breast cancer metastasis. Inhibition of LOX in MDA-231 suppresses focal adhesion kinase (FAK) signaling, resulting in reduced adhesive and migratory ability of the cancer cells (8). LOX and LOXL2 alter the tumor microenvironment by stiffening tissues through cross-linking collagen (10, 18), leading to FAK and PI3K signaling that promotes the invasive properties of cancer cells (10). The finding that LOX family members promote breast cancer metastasis by multiple mechanisms is consistent with data indicating that LOX/LOXL inhibition has major effects on metastasis in mouse models.

Increased HIF-1α levels are associated with increased metastasis and decreased survival in patients with breast cancer (2, 13). Our results demonstrate that HIF activity is a critical determinant of LOX family expression and prometastatic effects. Hypoxic breast cancers secrete various LOXs, including LOX, LOXL2,

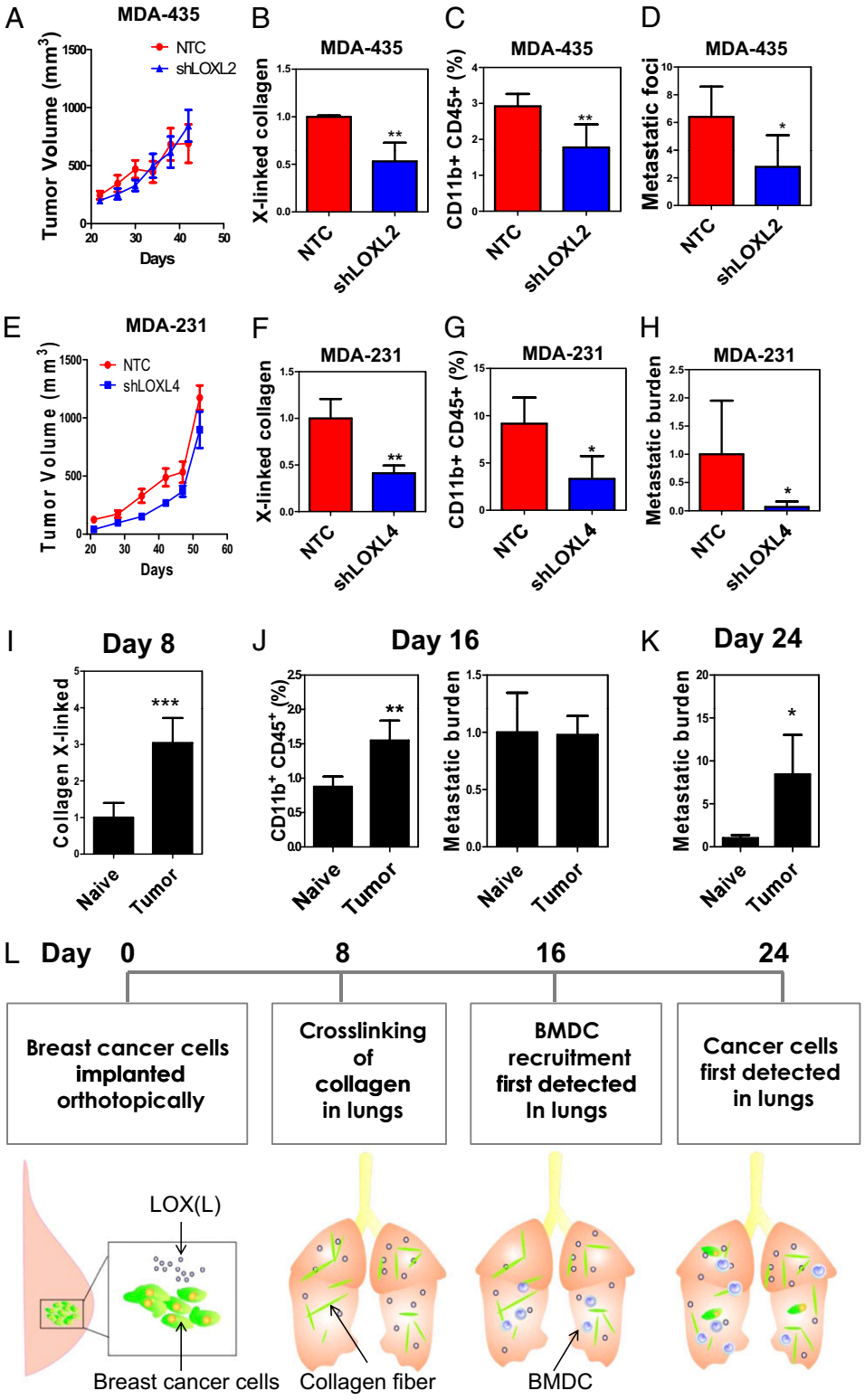

Fig. 5. LOX family members and breast cancer metastatic niche formation. (*A–D*) SCID mice received MFP injection of the indicated MDA-435 subclone. (*A*) Tumor volume was plotted against time. Cross-linked collagen fibers (normalized to NTC) (*B*), $CD11b^+CD45^+$ BMDCs (*C*), and metastatic foci (*D*) in the lungs were analyzed on day 42. Metastatic foci in the lungs were counted at a magnification of 20× per field (3 random fields per mouse). (*E–H*) Nonobese diabetic-SCID mice received MFP injection of MDA-231 subclones. (*E*) Tumor volume was plotted against time. (*F*) Cross-linked collagen fibers (normalized to NTC), (*G*) $CD11b^+CD45^+$ BMDCs, and (*H*) metastatic burden (determined by qPCR using human *HK2* gene primers and normalized to NTC) in the lungs were analyzed on day 52. (*I–L*) MDA-435 cells were injected into the MFP of SCID mice, which were euthanized 8, 16, or 24 d later. (*I*) Cross-linked collagen fibers were counted under polarized light and normalized to the naive control. (*J*) (*Left*) Percentage of $CD11b^+CD45^+$ BMDCs in the lungs of the mice on day 16 was analyzed by flow cytometry. (*Right*) Metastatic burden in the lungs of mice on day 16 was analyzed. (*K*) Metastatic burden in the lungs of mice on day 24 was analyzed by qPCR and normalized to naive control (mean ± SD; $n = 3$). $^*P < 0.05$, $^{**}P < 0.01$ vs. NTC; Student *t* test (mean ± SD; $n = 3$–4). (*L*) Summary of the mechanism and kinetics of metastatic niche formation in MDA-435 tumor-bearing mice.

and LOXL4, which cross-link collagen at sites of metastatic niche formation to promote recruitment of BMDCs, which stimulate lung colonization by breast cancer cells. Inhibition of HIF activity is sufficient to block metastatic niche formation, providing a mechanistic basis for including HIF inhibitors as components of multidrug regimens for breast cancer.

Materials and Methods

Primary Tumor Samples. Human breast cancer tissue and surrounding normal breast tissue were collected at the time of surgical resection at Queen Mary Hospital, University of Hong Kong. Use of human tissues was approved by the Institutional Review Board of the University of Hong Kong/Hospital Authority Hong Kong West Cluster.

Cell Culture Studies. The following are described in *SI Materials and Methods* and Table S1: construction of shRNA vectors, cell transfection, preparation of lentiviruses, and establishment of stably transfected cell lines; isolation and analysis of chromatin from cells; construction of pGL2 HRE luciferase reporters and cotransfection assays; real-time qPCR assays; Western blot assays; and in vitro collagen remodeling assays.

BMC Isolation and Invasion Assay. BMCs were harvested from mice by flushing femurs and tibias with PBS and sedimented through Histopaque (Sigma). Transwell inserts (Corning) were coated with matrigel (BD Biosciences) at 37 °C for 1 h. CM generated from MDA-231 or MDA-435 cells under 20% or 1% O_2 for 48 h was placed on the matrigel-coated insert for 16 h. CM was removed, and 1×10^6 freshly isolated BMCs or 3×10^5 naive breast cancer cells were resuspended in serum-free DMEM (CellGro) and seeded into the upper chamber. DMEM supplemented with 10% (vol/vol) FBS was placed in the bottom chamber as a chemoattractant. Cells were allowed to invade for 20 h. For BMC invasion assay, cells that invaded through the membrane were found in the lower chamber suspension. Invaded cells were counted by means of a hemocytometer or Countess automated cell counter (Invitrogen).

Orthotopic Implantation Studies. All animal protocols were approved by The Johns Hopkins University Animal Care and Use Committee. A total of 2×10^6 breast cancer cells resuspended in matrigel were injected into the second left MFP of 5- to 7-wk-old SCID or nonobese diabetic-SCID mice. Tumor growth was measured by calipers. Mice were euthanized, and the lungs were perfused with PBS. The left lung was inflated with low-melting-point agarose for fixation/paraffin embedding, and sections were subjected to H&E staining and immunohistochemical analysis. The right lung was used for DNA extraction and flow cytometry. Bioluminescent signals were detected by means of an IVIS Spectrum optical imaging device (Xenogen). Mice were injected i.p. with 100 mg/kg D-luciferin (Caliper Life Sciences) 5 min before imaging of primary tumor. Mice were euthanized, and their lungs and lymph nodes were excised for ex vivo imaging.

Lung Tissue Preparation, Genomic DNA Extraction, and Flow Cytometry Analysis. Lungs were digested with lysis buffer and proteinase K at 55 °C overnight, and genomic DNA was extracted with phenol-chloroform, precipitated with isopropanol, and washed with ethanol. Two hundred nanograms of genomic DNA was used for qPCR to quantify human *HK2* and mouse *18S* rDNA sequences. To prepare lung cells for flow cytometry analysis, tissues were minced and digested with 1 mg/mL type 1 collagenase (Sigma) at 37 °C for 30 min. Digested tissues were filtered through 70-μm cell strainers. Cells were incubated with Fc Block (BD Pharmingen) and then with peridinin chlorophyll protein-conjugated CD45 antibody (BD Pharmingen) and allophycocyanin-conjugated CD11b antibody (eBiosciences), and they were then subjected to flow cytometry analysis. Unstained control, CD45 single-stained, and CD11b single-stained cells were prepared in every experiment for gating. Dead cells were gated out by side-scatter and forward-scatter analysis.

Histochemistry. Lungs were fixed in 10% (vol/vol) formalin and washed with ethanol before paraffin embedding. Sections were dewaxed with xylene, and antigens were retrieved using citrate buffer. CD11b antibody (Novus Biologicals) and a LSAB+ System HRP kit (DAKO) were used for staining. Picrosirius Red (Sigma–Aldrich) was used for fibrillar collagen staining. Lung sections were stained with H&E to visualize metastatic foci.

ACKNOWLEDGMENTS. We thank Karen Padgett (Novus Biologicals Inc.) for providing antibodies against HIF-1β, HIF-2α, LOXL2, LOXL4, CD11b, and IgG control and Rashmi Bankoti, Sergio Rey, and Weibo Luo for advice. This work was supported by grants from the Emerald Foundation and National Institutes of Health (Grant U54-CA143868). D.M.G. was supported by NIH Grant T32-CA130840. G.L.S. is the C. Michael Armstrong Professor at The Johns Hopkins University School of Medicine. C.C.-L.W. is a Croucher Foundation Fellow.

1. Vaupel P, Mayer A, Höckel M (2004) Tumor hypoxia and malignant progression. *Methods Enzymol* 381:335–354.
2. Semenza GL (2010) Defining the role of hypoxia-inducible factor 1 in cancer biology and therapeutics. *Oncogene* 29:625–634.
3. Wang GL, Jiang BH, Rue EA, Semenza GL (1995) Hypoxia-inducible factor 1 is a basic-helix-loop-helix-PAS heterodimer regulated by cellular O_2 tension. *Proc Natl Acad Sci USA* 92:5510–5514.
4. Chintala S, et al. (2010) Se-methylselenocysteine sensitizes hypoxic tumor cells to irinotecan by targeting hypoxia-inducible factor 1α. *Cancer Chemother Pharmacol* 66: 899–911.
5. Chaffer CL, Weinberg RA (2011) A perspective on cancer cell metastasis. *Science* 331: 1559–1564.
6. Kaplan RN, et al. (2005) VEGFR1-positive haematopoietic bone marrow progenitors initiate the pre-metastatic niche. *Nature* 438:820–827.
7. Erler JT, et al. (2009) Hypoxia-induced lysyl oxidase is a critical mediator of bone marrow cell recruitment to form the premetastatic niche. *Cancer Cell* 15:35–44.
8. Erler JT, et al. (2006) Lysyl oxidase is essential for hypoxia-induced metastasis. *Nature* 440:1222–1226.
9. Csiszar K (2001) Lysyl oxidases: A novel multifunctional amine oxidase family. *Prog Nucleic Acid Res Mol Biol* 70:1–32.
10. Levental KR, et al. (2009) Matrix crosslinking forces tumor progression by enhancing integrin signaling. *Cell* 139:891–906.
11. Schietke R, et al. (2010) The lysyl oxidases LOX and LOXL2 are necessary and sufficient to repress E-cadherin in hypoxia: Insights into cellular transformation processes mediated by HIF-1. *J Biol Chem* 285:6658–6669.
12. Semenza GL, et al. (1996) Hypoxia response elements in the aldolase A, enolase 1, and lactate dehydrogenase A gene promoters contain essential binding sites for hypoxia-inducible factor 1. *J Biol Chem* 271:32529–32537.
13. Bos R, et al. (2003) Levels of hypoxia-inducible factor-1α independently predict prognosis in patients with lymph node negative breast carcinoma. *Cancer* 97: 1573–1581.
14. Bondareva A, et al. (2009) The lysyl oxidase inhibitor, beta-aminopropionitrile, diminishes the metastatic colonization potential of circulating breast cancer cells. *PLoS ONE* 4:e5620.
15. Payne SL, Hendrix MJ, Kirschmann DA (2007) Paradoxical roles for lysyl oxidases in cancer—A prospect. *J Cell Biochem* 101:1338–1354.
16. Görögh T, et al. (2007) Selective upregulation and amplification of the lysyl oxidase like-4 (LOXL4) gene in head and neck squamous cell carcinoma. *J Pathol* 212:74–82.
17. Kim Y, et al. (2009) Differential expression of the LOX family genes in human colorectal adenocarcinomas. *Oncol Rep* 22:799–804.
18. Barry-Hamilton V, et al. (2010) Allosteric inhibition of lysyl oxidase-like-2 impedes the development of a pathologic microenvironment. *Nat Med* 16:1009–1017.